



HAL
open science

A multi-period optimization model for the design of mass networks including conversion systems and gas storage models: application for hydrogen generation, distribution and storage

Thibaut Wissocq, Solène Le Bourdiec, Zoughaib Assaad

► To cite this version:

Thibaut Wissocq, Solène Le Bourdiec, Zoughaib Assaad. A multi-period optimization model for the design of mass networks including conversion systems and gas storage models: application for hydrogen generation, distribution and storage. *Computers & Chemical Engineering*, 2021, pp.107448. 10.1016/j.compchemeng.2021.107448 . hal-03314710

HAL Id: hal-03314710

<https://hal.science/hal-03314710>

Submitted on 22 Aug 2023

HAL is a multi-disciplinary open access archive for the deposit and dissemination of scientific research documents, whether they are published or not. The documents may come from teaching and research institutions in France or abroad, or from public or private research centers.

L'archive ouverte pluridisciplinaire **HAL**, est destinée au dépôt et à la diffusion de documents scientifiques de niveau recherche, publiés ou non, émanant des établissements d'enseignement et de recherche français ou étrangers, des laboratoires publics ou privés.



Distributed under a Creative Commons Attribution - NonCommercial 4.0 International License

A multi-period optimization model for the design of mass networks including conversion systems and gas storage models: application for hydrogen generation, distribution and storage

5 Thibaut Wissocq^{b,*}, Solène Le Bourdier^a, Assaad Zoughaib^b

^aEDF R&D, 77818 Moret-sur-Loing

^bMines ParisTech, Centre d'efficacité énergétique des systèmes, 5 rue Léon Blum, 91120 Palaiseau

Abstract

10 A multi-period mixed-integer-linear-programming problem for the design of mass networks is proposed in this paper. Design of mass networks, conversion systems and storages is done so as to minimize the capital expenses and operating costs and fulfill demand in resources. This work provides a detailed model of compressed gas storage, considering pressure state inside gas tank, compression costs and compressor design, which have not been considered before in a
15 linear model, with a discrete pressure scale. The performance of the model is assessed on a hydrogen network design problem, including renewable electricity, electrolyzer design and hydrogen storage. The share of renewable electricity use increases from 60% to 90% with hydrogen storage. Different compressed gas
20 storage linearized models are compared with different pressure scales and the linearization error is assessed. The introduction of discrete intermediate pressures reduces the committed error on compressor power and operating costs, due to the linearization.

Keywords: MILP, multi-period, hydrogen network, compressed gas storage,
25 electrolyzer

*Corresponding author

Email address: thibaut.wissocq@edf.fr, thibaut.wissocq@mines-paristech.fr
(Thibaut Wissocq)

Highlights

- A multiperiod MILP problem is developed for the optimal design of hydrogen network and storage.
- A new linearized compressed gas storage model is proposed, considering compression energy costs.
- A discretized pressure scale is introduced.
- Computational and precision performances are assessed on a case study.

1. Introduction

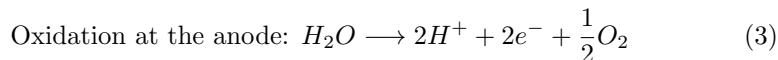
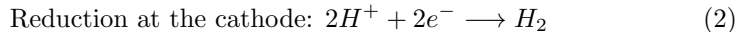
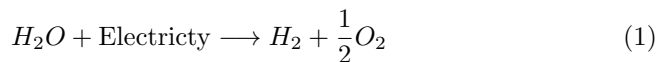
1.1. Context

The share of renewable resources in final energy consumption is increasing in Europe since 2004 and a target of 32% is set by 2030 (Eurostat, 2020). In this way, design and development of multi-energy systems appear to be an opportunity. They consist of the integration between several energy networks of different nature: electricity, gas, heating and cooling. These energy sectors are traditionally designed separately even though close interactions can take place. For instance, technologies such as heat pumps, Combined Heat and Power (CHP) or gas turbines couple heat and electricity networks. Heat pumps consumes electricity and can supply energy to a heat network while CHP can produce both electricity and heat. Moreover, one of the main drawbacks of renewable electricity (wind, photovoltaic) is their intermittency. They are hardly monitored, their production must be used instantaneously and matching electricity supply and demand is mandatory. The utilization of electric storages like lithium-ion batteries can be a solution but they are mainly short-term solutions (Kusko and DeDad, 2005; Smith et al., 2008; Walker et al., 2016). They hardly store electricity for a long-period and it requires costly investments in case of seasonal storage. The power-to-gas technologies can also tackle this issue. The idea is to convert electricity into gas. The surplus of electricity from renewable resources can be converted into hydrogen (H_2 conversion by electrolyzer)

and into natural gas (methanation). Moreover, the conversion into natural gas
 55 benefits the already existing distribution gas networks and storages. Actually,
 the total world gas storage capacity exceeds largely the total world power from
 wind and solar (Götz et al., 2016), thus, power-to-gas can provide flexibility
 and enhance the integration of renewable intermittent resources, using gas as
 an energy carrier. Actually, hydrogen is characterized by a high energy den-
 60 sity (three times higher than liquid hydrocarbon based fuels) and low losses in
 transportation, thus it is seen as an efficient energy carrier (Walker et al., 2016;
 Mazloomi and Gomes, 2012).

1.2. Hydrogen production

Hydrogen can be produced through several pathways. The most popular
 65 is steam-methane reforming (SMR) (almost 48% of total hydrogen production
 (Mazloomi and Gomes, 2012)) from fossil fuels but it generates greenhouse gases
 (CO, CO₂). This pathway produces non-renewable hydrogen, generally referred
 as ‘grey hydrogen’. The other pathway is water electrolysis, providing a high
 purity of hydrogen and is considered to be a promising technology to mass
 70 produce hydrogen (Walker et al., 2016). The water is decomposed into oxygen
 and hydrogen by means of a continuous electric current supplied by a power
 source, a battery or a cell, connected by electrodes to the water. The electricity
 can be produced by renewable resources (wind or solar) making the hydrogen
 renewable (and called ‘green hydrogen’). The main reactions are equations (1)
 75 to (3):



Two main types of electrolyzers are used: alkalyne electrolyzers and Polymer Electrolyte Membrane (PEM) electrolyzers (Abdin et al., 2015, 2017). Alkalyne water electrolysis is the most used in industry nowadays because they are cheaper. However, hydrogen produced from PEM has some advantages: the hydrogen produced is highly pure and there are no hazardous chemicals contrary to alkalyne electrolyzers. Moreover, they can reach higher current density values, above 2 A/cm², improving the yield and its profitability. Finally, they can also operate in a large power range, from 10% to 100% of the nominal power or even higher (Barbir, 2005; E&E Consultant et al., 2014). Different degrees of complexity can be found in literature about PEM electrolyzer modelling. The first PEM models of electrolyzer were published from 2002 and focused on steady-state behavior (Onda et al., 2002; Khan and Iqbal, 2005; Busquet et al., 2004; Kélouwani et al., 2005; Görgün, 2006). However, given the intermittency and the variability of renewable power sources, dynamic behavior should be taken into account for detailed model. Dynamic behaviour consideration requires more comprehensive models, including differential equations, thus their resolution increases the model complexity (Falcão and Pinto, 2020; Carmo et al., 2013; Olivier et al., 2017). Dynamic model of PEM has been studied in the literature (Abdin et al., 2017; Carmo et al., 2013; Olivier et al., 2017; Marangio et al., 2011; Lebbal and Lecœuche, 2009; Nie et al., 2009; Nie and Chen, 2010; Awasthi et al., 2011; García-Valverde et al., 2012; Gabrielli et al., 2016). These theoretical models are in most cases confronted to experimental data. They take into account activation losses, based on Butler-Volmer kinetic laws (Abdin et al., 2017; Marangio et al., 2011; Lebbal and Lecœuche, 2009). Recently Falcão and Pinto (2020) presented a review of PEM electrolyzers modelling, detailing the technology basic principles. PEM modelling improves the understanding of the electrolyzer and helps the prediction of their behaviour. However, due to model complexity, simpler models are often used in large-scale energy problems, like power-to-gas problems (Reuß et al., 2019). Electrolyzers are defined by its efficiency, most of the time static and independent of operating conditions. Its efficiency relates of the conversion of water into hydrogen and oxygen, with

electricity. In Kélouwani et al. (2005); Zervas et al. (2008), the electrolyzers is
110 modelled using conversion factors, directly provided by the manufacturers and
a comparison between simulation and experiments are conducted.

1.3. Hydrogen in supply chain design

Electrolyzer modelling is also covered in hydrogen supply chain design topics
115 (Li et al., 2019; Yue et al., 2014; Moreno-Benito et al., 2017; Van Den Heever and
Grossmann, 2003; Martín and Grossmann, 2011). Almansoori and Shah (2006,
2009) presented an optimization model of a future hydrogen supply chain. This
model was first static and then extended to multiperiod (long term evolution and
infrastructure design). Production pathways and transportation networks were
120 optimized under the economic aspect. Li et al. (2020) developed a MILP model
of a hydrogen supply network. Feedstock supply (from SMR, electrolysis and
biomass gasification), production facilities and transportation were considered
to minimize the cost of hydrogen. The model was static and did not consider
hydrogen storage. Also, Chahla and Zoughaib (2019) developed a methodol-
125 ogy for the integration of biomass conversion into a hydrogen energy system in
a non-cooperative governance, where the industrial actors search to maximize
their own interest. The model was also static and without hydrogen storage.
Samsatli and Samsatli (2015) developed a MILP model to design the hydrogen
network considering hourly hydrogen demand and electricity from wind tur-
130 bines. Different conversion technologies, modelled by a conversion factor were
modelled in order to supply hydrogen. Different type of storages can also be
used: underground, compressed gas at 200 bars, liquid and metal hydride. A
non uniform time discretization is used in order to address the tractability chal-
lenge. Most of papers tackling the multiperiod problem of hydrogen demand
135 and the variability issue of renewable resources integrate compressed hydrogen
storage. This is one of the most mature technology for hydrogen storage com-
pared to metal hydride and cryogenic (Barthelemy et al., 2017). In these papers,
compression costs are included in the storage cost but this cost is independent

of the pressure inside the storage (Kélouwani et al., 2005; Zervas et al., 2008;
140 Almansoori and Shah, 2009; Samsatli and Samsatli, 2015; Ruiming, 2019) and
it does not allow compressor design. As far as the authors know, the question
of designing the compressor for storages is barely considered in power-to-gas
topics and it has not been considered yet in a linear model.

This should be considered because:

145

- The investment cost of a compressed storage depends also on the size
(power) of the compressor.
- The compression mass flow depends on compressor sizing. Mass flow is
limited to its maximal power.
- 150 • The compression energy need depends on pressure changes, thus operating
costs depend on pressure changes.
- Computing compression energy consumption allows us to estimate com-
pressor cooling, thus estimate the recoverable waste heat potential.

However, the equations describing the behaviour of compression gas storages
155 are non-linear, particularly the equation of state and the computation of work
compression. This adds to the difficulties in solving by reducing the computa-
tional tractability, which explains the lack of compression modelling.

1.4. Goal of this paper

160 Therefore, this paper proposes a linearized model of compressed gas storage
based on a pressure discretization. This model is included into a multi-period
optimization problem for the design of mass and energy networks, extending the
work of Ghazouani et al. (2017). Generic models of conversion systems are also
included in the model. A Mixed-Integer-Linear-Programming (MILP) problem
165 is defined in order to design storages, conversion systems and networks consid-
ering mass and energy demand. The objective function is the minimization of

the total costs (investment and operating costs). The problem is applied to a hydrogen case study, inspired of Samsatli and Samsatli (2015).

1.5. Structure of paper

170 This paper is structured as follows. The problem statement is presented in section 2 and the equations of the MILP problem are detailed in section 3. Finally, the model is applied to a hydrogen case study in section 4. It deals with a hydrogen demand, varying in time. The hydrogen demand is fulfilled thanks to an electrolyzer using electricity produced by wind turbines and the grid. The
 175 compressed hydrogen storage linear model is also used. An evaluation of the approximation error due to the linearization is done. Some perspectives of the current work are presented in section 5.

2. Problem statement

2.1. Superstructure definition

180 This paper presents a multi-period optimization model for the design of multi mass networks, conversion and storage systems between different clusters. Each cluster represents an industrial actor and can exchange resources (energy, water, hydrogen, ...) through mass networks to other clusters of the territory.

Each cluster $c \in \mathcal{C}$ can contain different elements:

- 185 • Process sources ($j_r \in J_p$). They correspond to material resources (ex: H_2) or effluents (ex: water) that are available and can be reused in the process or in the territory. They are defined by their type $r \in \mathcal{R}$, a given mass flow rate $L_{c,j_r,t}$ for each period of time $t \in \mathcal{T}$.
- Process sinks ($i_r \in I_p$). They correspond to process units that require a
 190 given mass flow rate ($G_{c,i_r,t}$) for each material type $r \in \mathcal{R}$ and each period of time $t \in \mathcal{T}$.
- Variable sources ($j_r \in J_v$) are available in a cluster in order to satisfy process sink requirements. Their mass flow rate $L_{c,j_r,t}^v$ are unknown for

each material type $r \in \mathcal{R}$ and each period of time $t \in \mathcal{T}$. They are
195 variables to be optimized. They represent the input flow of systems such
as storages, conversion systems or the purchase of a resource, with an
associated cost.

- Variable sinks ($i_r \in I_v$) are available in a cluster in order to discard re-
sources that cannot be used directly in a cluster. Their mass flow rate
200 $G_{c,i_r,t}^v$ are unknown for each material type $r \in \mathcal{R}$ and each period of time
 $t \in \mathcal{T}$. They are variables to be optimized. They represent the output
flow of systems such as storages, conversion systems or resource disposal
at a certain cost.

205 More sophisticated systems can be defined, based on the definition of sources
and sinks:

- Mass storages ($s_r \in S$), created by the association of a variable source and
sink ($(j_r, i_r) \in J_v \times I_v$). They can be daily or seasonal storages. They are
characterized by capital and operating costs. This element is described
210 further in details in 3.3.
- Conversion systems ($sc \in SC$), created by the association of variables
sources and sinks ($(j_r, i'_r) \in J_v \times I_v$). They are used to convert resources
in other resources (for example: electrolyzer and H_2), with an electrical
demand or production. This element is described further in details in 3.5.

215 Resources can be exchanged inside a cluster (between different sinks, sources
and technologies) or between different clusters through a dedicated mass net-
work. This network is characterized by an investment cost (proportional to the
length of a path).

220 2.2. Optimization target

The target of the study/analysis is to determine optimal results for:

- The mass flow rate between the different sources and sinks (inside a cluster or between different cluster) ;
- the network topology ;
- 225 • the storage evolution with time ;
- the mass storage design ;
- the conversion systems design ;
- the investment decisions such as the localization of different technologies.

So as to minimize the Total Annualized Costs (CAPEX+OPEX) while sat-
 230 isfying the resource needs of each cluster in a territory.

3. Model formulation

3.1. Mass balance inside a cluster

Inside each cluster $c \in \mathcal{C}$, the mass flow requirement $G_{c,i_r,t}$ of each sink $i \in I$ has to be met for a sink i_r (equation (4)) and for a variable sink i_r (equation (5)):

235

$$\forall t \in \mathcal{T}, \forall i_r \in I_p, \forall r \in \mathcal{R} \quad G_{c,i_r,t} = \sum_j L_{c,ij_r,t} + \sum_j L_{c,ij_r,t}^v \quad (4)$$

$$\forall t \in \mathcal{T}, \forall i_r \in I_v, \forall r \in \mathcal{R} \quad G_{c,i_r,t}^v = \sum_j L_{c,ij_r,t} + \sum_j L_{c,ij_r,t}^v \quad (5)$$

where $L_{c,ij_r,t}$ is the mass flow from a source j_r to the sink i_r and $L_{c,ij_r,t}^v$ is the mass flow from a variable source j_r to the sink i_r .

In the same way, the mass flow leaving a source j_r (equation (6)) and a
 240 variable source j_r (equation (7)) is equal to its total flow rate:

$$\forall t \in \mathcal{T}, \forall j_r \in J_p, \forall r \in \mathcal{R} \quad L_{c,j_r,t} = \sum_i L_{c,ij_r,t} + \sum_i L_{c,ij_r,t}^v \quad (6)$$

$$\forall t \in \mathcal{T}, \forall j_r \in J_v, \forall r \in \mathcal{R} \quad L_{c,j_r,t}^v = \sum_i L_{c,ij_r,t} + \sum_i L_{c,ij_r,t}^v \quad (7)$$

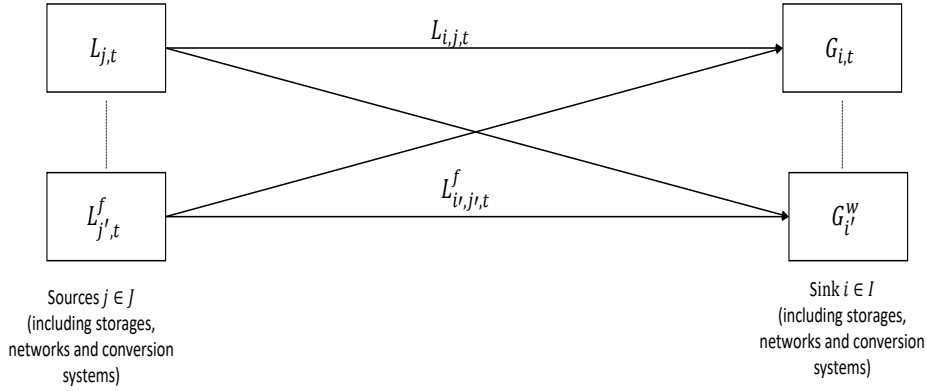


Fig. 1. Superstructure for mass balance in a cluster.

Figure 1 represents the superstructure and the mass balance inside a cluster between sources and sinks.

3.2. Mass networks

245 Exchange of material between industries, modelled by the clusters, is realized through mass networks. A mass network $(j_r, i_r) = m \in M_{net}$ of a resource $r \in \mathcal{R}$ is modelled as a variable source $j_r \in J_v$ and a variable sink $i_r \in I_v$ inside each cluster $c \in \mathcal{C}$ of the problem. We note $c_m \in \mathcal{C}_m$ the subset of clusters interacting with the mass network m . The variable source represents the matter
 250 provided by the network to the cluster and the variable sinks represent the matter leaving the cluster and entering into the network. Therefore, mass exchange between a cluster and a mass network are defined by the set of equations (4) to (7). Specific equations for the mass network are defined.

We assume that there is no mass accumulation in the network : the matter entering into the network is instantaneously consumed by a cluster (equation (8)):
 255

$$\forall t \in \mathcal{T}, \forall (j_r, i_r) = m \in M_{net}, \sum_{c \in \mathcal{C}_m} G_{c,i_r,t}^v = \sum_{c \in \mathcal{C}_m} L_{c,j_r,t}^v \quad (8)$$

A mass network m is defined by a certain number of authorized paths $p_m \in P$, connecting two clusters. To each path $p \in P$ is associated an arbitrary direction $\delta_p = \pm 1$, orienting the path. We define also the set \mathcal{P}_c corresponding

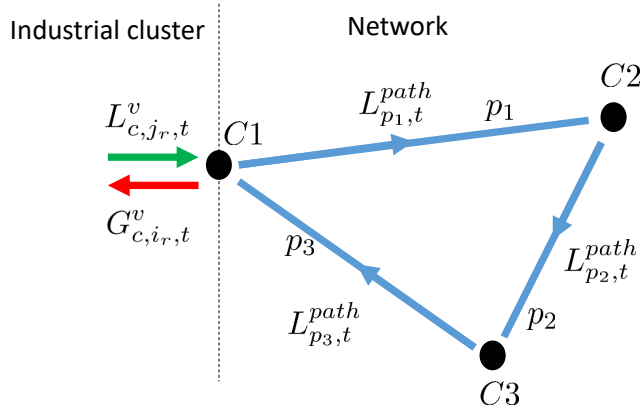


Fig. 2. Illustration of a mass network

to the all paths passing through a cluster c :

$$\forall t \in \mathcal{T}, \forall c \in \mathcal{C}, \sum_{p \in \mathcal{P}_c} L_{p,t}^{path} \delta_p = G_{c,i_r,t}^v - L_{c,j_r,t}^v \quad (9)$$

260 Where $L_{p,t}^{path}$ is the flow rate (which can be positive or negative depending on the orientation of the path) through the path p at the time t (figure 2 and equation (9)) is applied to each cluster.

For example, in figure 2, three clusters are present, and one mass network connects each them. Three paths are possible: from C1 to C2 (p_1), from C1
 265 to C3 (p_3) and from C2 to C3 (p_2). $G_{c,i_r,t}^v$ is the mass flow entering into the network at the cluster c_1 (or leaving the cluster c_1 through a waste sink) and $L_{c,i_r,t}^v$ is the mass flow leaving the network at the cluster c_1 (or entering into the cluster c_1 through a fresh source).

270 Binary variables are introduced in order to detect whether a path is used in a mass network through big-M equations (equations (10) and (11)):

$$\forall p \in \mathcal{P}, \forall t \in \mathcal{T}, L_{p,t}^{path} - \Omega \cdot b_p \leq 0 \quad (10)$$

$$\forall p \in \mathcal{P}, \forall t \in \mathcal{T}, L_{p,t}^{path} + \Omega \cdot b_p \geq 0 \quad (11)$$

where Ω is a great number (the maximum capacity of the paths for example)

3.3. Mass storage formulation

Mass storage $((i_r, j_r) = s_r \in S)$ is modelled by a couple of a variable sink j_r and of a variable source i_r for the resource r in a cluster c . We define the sets I_s and J_s corresponding to the subsets of variables sources and sinks belonging to a storage. The storage is modelled by three main positive variables: the flow entering the storage $G_{c,j_r,t}^v$, the output flow $L_{c,i_r,t}^v$ and the amount of mass stored at the end of the period $S_{c,s_r,t}$. We assume that the steady state is established at each period.

The storage evolution is given by equation (12) where δt_t corresponds to the duration of a period $t \in \mathcal{T}$:

$$S_{c,s_r,t+1} = S_{c,s_r,t} + \left(G_{c,j_r,t}^v - L_{c,i_r,t}^v \right) \cdot \delta t_t \quad \forall (i_r, j_r) = s_r \in S, \forall t \in \mathcal{T} \quad (12)$$

The maximum capacity of a storage is given by equation (13):

$$Max-S_{c,s_r} \geq S_{c,s_r,t} \quad \forall (i_r, j_r) \in S, \forall t \in \mathcal{T} \quad (13)$$

Big-M formulation are used in order to define binary variables (equations (14) and (15)), defining the existence of inlet and outlet flows:

$$G_{c,j_r,t}^v \leq b_{c,j_r,t}^{in} \cdot \Omega \quad \forall j_r \in J_s, \forall t \in \mathcal{T} \quad (14)$$

$$L_{c,i_r,t}^v \leq b_{c,i_r,t}^{out} \cdot \Omega \quad \forall i_r \in I_s, \forall t \in \mathcal{T} \quad (15)$$

Emptying or filling a mass storage simultaneously is forbidden (equation (16)):

$$b_{c,i_r,t}^{out} + b_{c,j_r,t}^{in} \leq 1 \quad \forall s_r = (i_m, j_m) \in S, \forall t \in \mathcal{T} \quad (16)$$

A binary is used to detect if a mass storage (i_r, j_r) is used (equation (17)):

$$Max-S_{c,s_r} \leq b_{c,s_r}^S \cdot \Omega \quad \forall s_r \in S \quad (17)$$

3.4. Compressed gas storage

290 3.4.1. Limitations of the incompressible storage model

The equations presented above (equations (12) to (17)) are adapted for incompressible mass storage. They are not sufficient to model compressed gas storage:

- The discharge pressure impacts the compression work, thus the operating costs.
- The power input of the compressor depends on the intake flow and on the discharge pressure.
- The investment cost of a compressed gas storage depends on the nominal power of the compressor

295
300 Therefore, an extended model is proposed in this paper in order to consider the gas compressibility, the compressor design and evaluate the compression costs. This model includes the computation of the gas pressure inside the storage, the volume design and the energy demand for the gas compression. We define the subset $S_g \subset S$ corresponding to the set of compressed gas storage.

305 The main assumptions are:

- The gas is an ideal gas, with a constant heat capacity ratio γ .
- The gas is compressed by a multi-stage compressor with intercooling.
- The pressure ratio is identical for all the stages (and depends on the number of stages).
- The temperature T_{s_g} inside the storage is constant.

310 The mechanical power needs for the compression per mass flow rate w_{s_g} is expressed by equation (18):

$$w_{s_g} = \frac{NR\gamma T}{M(\gamma - 1)} \left(\left(\frac{P_{s_g}}{P_1} \right)^{\frac{\gamma-1}{N\gamma}} - 1 \right) \quad \forall s_g \in S_g \quad (18)$$

where N is the number of compression stages, P_1 is the pressure at the inlet and P_{s_g} is the pressure inside the storage.

315

The highest pressure inside the storage can be found through the application of the ideal gas law:

$$P_{s_g} V_{s_g} = \frac{Max_{S_{c,s_g}} RT_{s_g}}{M_g} \quad \forall s \in S_g \quad (19)$$

These two equations (18) and (19) are non-linear because of the presence of the power function and because of the multiplication of several variables between them: pressure, volume and the mass flow rate. Linearization of these equations are developed in section 3.4.2.

320

3.4.2. Mathematical linearized model

A pressure discretization is introduced: each compressed gas storage is defined by a pressure scale and equation (18) is pre-computed on each pressure interval. The mean value is used for pre-computed the mechanical compression work on each interval (equation (20)). Figure 3 presents and compares the value for the evolution of mechanical compression according to the pressure inside the storage (assuming the gas is hydrogen and there are four compression stages) with the discrete mean values computed by equation (20). This discretization can drive to another approximation. The pressure inside the storage can vary during a time step, leading to a shift for the discrete pressure between two consecutive time steps and the mean value used can be far from the actual value. Therefore, the computation of the mechanical work will consider two consecutive time steps in order to reduce this approximation. Depending on the pressure inside the storage, the corresponding mean value will be used. Indeed, the pressure inside the storage can be under or over-estimated, that can lead to errors in the computation of work. Thus, a trade-off is necessary between the

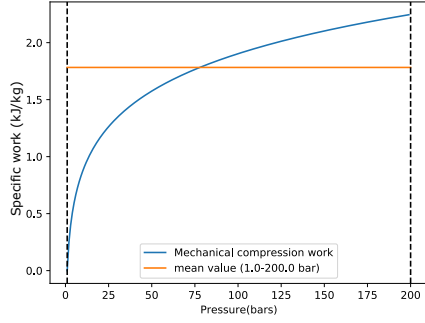
330

335

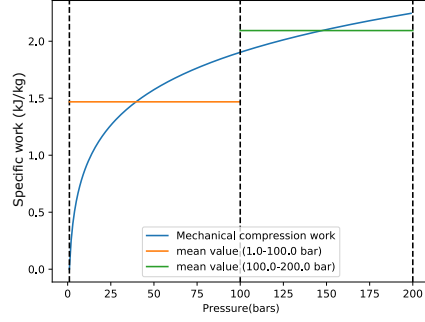
discretization and the accuracy level.

$$\widetilde{w_{c,s_g,p}} = \frac{1}{P_{p+1} - P_p} \int_{P_p}^{P_{p+1}} \frac{NR\gamma T}{M(\gamma - 1)} \left(\frac{p}{P_1}^{\frac{\gamma-1}{N\gamma}} - 1 \right) dp \quad (20)$$

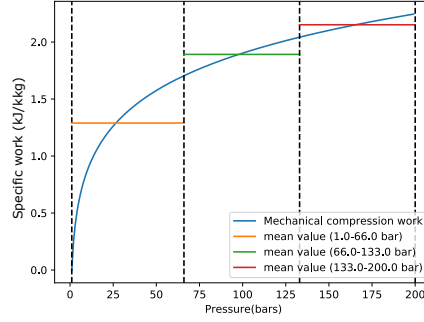
$$\forall s_g \in S_g, \forall p \in \{P_0, P_1, \dots, P_{N_{s_g}-1}\}$$



(a) 1 pressure interval



(b) 2 pressure intervals



(c) 3 pressure intervals

Fig. 3. Discretization of the mechanical work for compression

The superstructure for the compressed gas storage is presented in figure 4:
 340 the gas volume is fictively divided in several storages with the same volume and
 with the same amount of gas stored. Each fictive storage is defined by its own
 pressure interval and a dedicated flow rate. Binary variables are then introduced
 for each fictive storage and are used to determiner which pressure interval and
 which fictive storage are used. In other words, this binary is equal to 1 if the
 345 pressure inside the storage corresponds to this fictive storage.

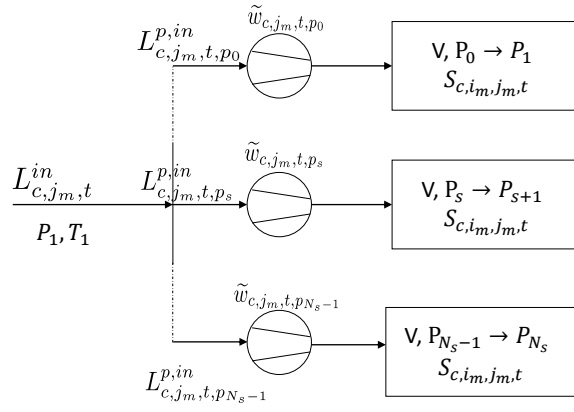


Fig. 4. Superstructure for the compressed gas storage.

The mass flow rate entering the storage is hence discretized through the pressure discretization for two consecutive time steps (subscript before/after) (equations (21) to (24)):

$$G_{c,i,t}^v = \sum_{p_s \in P} L_{c,s,t,p_s}^{p,in,before} \quad \forall t \in \mathcal{T}, \forall (i,j) = s \in S_g \quad (21)$$

$$G_{c,i,t}^v = \sum_{p_s \in P} L_{c,s,t,p_s}^{p,in,after} \quad \forall t \in \mathcal{T}, \forall (i,j) = s \in S_g \quad (22)$$

$$L_{c,s,t,p_s}^{p,in,before} \leq \Omega \cdot bin_{s,t,p}^P \quad \forall t \in \mathcal{T}, \forall s \in S_g \quad (23)$$

$$L_{c,s,t,p_s}^{p,in,after} \leq \Omega \cdot bin_{s,t+1,p}^P \quad \forall t \in \mathcal{T}, \forall s \in S_g \quad (24)$$

$$\sum_{p \in P} bin_{s,t,p}^P = 1 \quad \forall t \in \mathcal{T}, \forall s \in S_g \quad (25)$$

The energy required at the compressor is computed using the two pressure states before and after filling the storage with gas in order to consider pressure

350

changes (equation (26)):

$$\begin{aligned}\tilde{w}_{s,t}^{comp} &= \sum_{p \in P} \tilde{w}_{c,s,t,p} = \frac{1}{2} \sum_{p \in P} L_{c,s,t,p_s}^{p,in,after} \widetilde{w}_{c,s,p} \\ &\quad + \frac{1}{2} \sum_{p \in P} L_{c,s,t,p_s}^{p,in,before} \widetilde{w}_{c,s,p}\end{aligned}\quad (26)$$

$$\forall t \in \mathcal{T}, \forall s \in S_g$$

Big-M constraints are introduced in order to identify the pressure interval inside the storage, *via* the ideal gas law (equation (27)). $S_{c,s,t}$ is the total amount stored, V_s is the volume of the storage and Ω is a great number. If $bin_{s,t,p}^P = 1$ during a time step, the amount of mass is restricted by the two equations (right hand side of the equations), the pressure inside the storage belongs to the p^{th} interval, the corresponding mean value of compression energy is used and the ideal gas law can be applied. When $S_{c,s,t}$ reaches an infimum or supremum defined by the RHS of equation (27), the pressure interval changes.

$$\begin{aligned}S_{c,i_m,j_m,t} &\geq \frac{pV_{i_m,j_m}}{M_m RT_{i_m,j_m}} - (1 - bin_{i_m,j_m,t,p}^P) \cdot \Omega \\ S_{c,i_m,j_m,t} &\leq \frac{pV_{i_m,j_m}}{M_m RT_{i_m,j_m}} + (1 - bin_{i_m,j_m,t,p}^P) \cdot \Omega\end{aligned}\quad (27)$$

$$\forall t \in \mathcal{T}, \forall (i_m, j_m) \in S_g, \forall p \in P$$

The storage volume is designed by equation (28), using the minimum of gas stored at the lowest pressure and by the maximum of gas stored at the highest pressure (equation (28)).

$$\begin{aligned}Max_S_{c,s} &= \frac{P_{s,N_s} V_s}{RT_s} \quad \forall s \in S_g \\ Min_S_{c,s} &= \frac{P_{s,0} V_s}{RT_s} \quad \forall s \in S_g\end{aligned}\quad (28)$$

The nominal power of the compressor is computed by the equation

$$P_s \geq \tilde{w}_{s,t}^{comp} \quad \forall t \in \mathcal{T}, \forall s \in S_g \quad (29)$$

3.5. Conversion system formulation

Conversion systems consist of process that convert resources (electricity, material) into other resources. They are modelled and introduced into the problem.

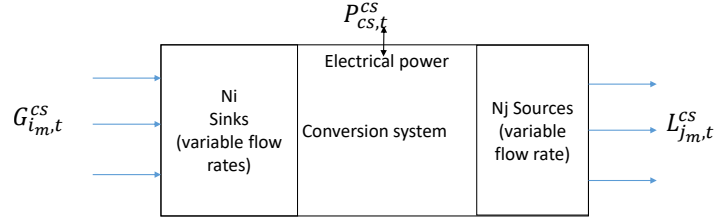


Fig. 5. Representation of a generic conversion system.

The concept of sinks and sources is re-used for their modelling. A schematic representation of a conversion system is presented on figure 5. For each conversion system $(i, j) = cs \in CS$ is associated a number N_i of variable sinks
 370 (resource input), a number N_j of variable sources (resource production) and electrical power is associated to the conversion (positive or negative, depending if the conversion system generates or consumes electricity). The mass flow rates and electrical power are variables of the system, to be designed. We define also the subsets I_{cs} and J_{cs} corresponding to the sinks and the sources associated
 375 to a conversion system cs . For example for an electrolyzer, as used in the case study 4, water and electricity will be the variable sinks while hydrogen and oxygen will be the variable sources of the conversion system.

The behaviour of the conversion system in nominal mode can be represented by a generic linear function, linking all the variables of the system (equation (30)):
 380

$$\forall t \in \mathcal{T}, F(L_{c,j,t}^v, G_{c,i,t}^v, P_{cs,t}) = 0 \quad (30)$$

The conversion system is modelled as a grey box and is characterized by different ratio between a reference source j_f and the other sources j and sinks i :

$$L_{c,j,t}^v = r s_j L_{c,j_f,t}^v \quad \forall t \in \mathcal{T}, \forall j \in J_{cs} \quad (31)$$

$$G_{i,t}^v = r s_i L_{c,j_f,t}^{cs} \quad \forall t \in \mathcal{T}, \forall i \in I_{cs} \quad (32)$$

385 The power consumption or generation of the conversion system is given by

equation (33):

$$P_{cs} \geq P_{cs,t} \quad \forall t \in \mathcal{T}, \forall cs \in CS \quad (33)$$

A binary variable is also defined in order to detect the use or not of the conversion system (equation (34)):

$$P_{cs} \geq \Omega b_{cs} \quad \forall cs \in CS \quad (34)$$

3.6. Electricity balance

390 Electricity consumption and production of each cluster is also taken into account. The electricity consumption EC_t is aggregated from the consumption of the compressed gas storage S_g and the conversion systems consuming electricity SC_c .

$$EC_t = \sum_{s \in S_g} \tilde{w}_{s,t}^{comp} + \sum_{sc \in SC_c} P_{sc,t} \quad \forall t \in \mathcal{T} \quad (35)$$

The electricity production EP_t is aggregated from the electrical sources in
395 all the clusters and from the conversion systems generating electricity SC_p

$$EP_t = \sum_{c \in \mathcal{C}} EP_{c,t}^c + \sum_{sc \in SC_p} P_{sc,t} \quad \forall t \in \mathcal{T} \quad (36)$$

The electricity balance is achieved at the territory scale. Each cluster is connected to the grid and can buy electricity from it if necessary (equation (37)), with a limitation (equation (38)).

$$EP_t + EP_t^{res,in} = EC_t + EC^{res,out} \quad \forall t \in \mathcal{T} \quad (37)$$

$$EP_t^{res,out} \leq EP_t^{limit} \quad \forall t \in \mathcal{T} \quad (38)$$

400 3.7. Objective Function

The objective function is the minimization of the total actualized cost (TAC) including the investment costs $CAPEX$ and the operational costs $OPEX$ (equation (39)), assuming an actualization ratio r_a and a number of operating years

N_y :

$$\min \left(CAPEX + \sum_{y=1}^{N_y} \frac{OPEX}{(1+r_a)^y} \right) \quad (39)$$

405 where in the investment costs are included the cost of the conversion systems, the storage units and the pipes between different clusters (equation (40)):

$$\begin{aligned} CAPEX = & \sum_{cs \in CS} (C_{cs}^u b_{cs} + C_{cs}^v P_{cs}) \\ & + \sum_{s \in S} (C_s^u b_s + C_s^v S_s + C_s^p P_s) + \sum_{p \in Paths} C_p^u d_p b_p \end{aligned} \quad (40)$$

The costs for storage units and conversion systems are separated between a fixed cost per unit (C_{cs}^u and C_s^u) and variable cost depending on the size of the unit (C_{cs}^v , C_s^v and C_s^p). Storage cost depends on the maximal capacity and on
410 the compressor nominal power. The cost for a conversion system unit depends on the electrical nominal power. For the pipes, a nominal cost per distance C_p^u is assigned for each pipe p . This cost is assumed to be independent of the mass flow rate.

415 The operating costs include the cost of fresh material C_j^v , waste disposal C_i^v and electricity C_t^e (equation (41)):

$$\begin{aligned} OPEX = & \sum_{t \in \mathcal{T}} \sum_{c \in \mathcal{C}, j \in J_v} C_j^v L_{c,j,t}^v \\ & + \sum_{t \in \mathcal{T}} \sum_{c \in \mathcal{C}, i \in I_v} C_i^v G_{c,i,t}^v + \sum_{t \in \mathcal{T}} C_t^e EP_t^{res} \end{aligned} \quad (41)$$

4. Case study

4.1. Presentation

The model developed in section 3 is applied to the problem of designing
420 a hydrogen network, its supply via electrolyzers and hydrogen storage sizing. The territory is composed of three clusters associated with a hydrogen demand, distanced at 1 kilometre. A hydrogen network is introduced, with a linear cost

of 500€/m (Ghazouani, 2016). The objective of the case study is to demonstrate the relevance and pertinence of the model developed in this paper. Data
 425 is inspired from Samsatli and Samsatli (2015). The cluster’s hydrogen demand fluctuates between weekdays, weekend and seasons. Wind turbines are present in the cluster C1 and generates electricity, fluctuating between the seasons and during a day. In order to construct the time dependent dataset (hydrogen demand and electricity production), data from 8 typical days is used: 2 days
 430 (weekdays and weekend) for the four seasons winter, spring, summer and autumn. Each weekday is repeated 65 times and each week-end days is repeated 26 times. Each day is discretized into a period of one hour. In this way, the problem contains $\mathcal{T} = 8736$ periods representing each hour of a year (52 weeks).

435 An electrolyzer to be designed is placed in cluster C1. It will convert the available electricity in the territory into hydrogen, with a nominal ratio. The characteristics (ratio, cost) of the PEM electrolyzer are detailed in table 1. The water consumption for converting electricity in hydrogen is not taken into account here, assuming that water is always available, with a neglected cost and
 440 oxygen production is also not taken into account. We focus here on the hydrogen demand and the electricity consumption but the model could easily be extended, considering water and oxygen ratios, water availability and oxygen demand (which could provide income). The electrolyzer operating cost corresponds to the electricity consumption, when local electricity production is not
 445 sufficient to cover the demand. Therefore, complementary electricity has to be imported from the grid. Electricity prices are detailed in figure 6.

Table 1

Characteristics of the conversion system PEM electrolyzer. Data from Samsatli and Samsatli (2015); Won et al. (2017); Jacobs (2016); Gorre et al. (2020) and own calculations

	Electric ratio $/H_2$ (kg/kWh)	CAPEX (fixed cost in €)	CAPEX (variable cost in €/kW)
Electrolyzer	18.10^{-3}	3.10^6	500

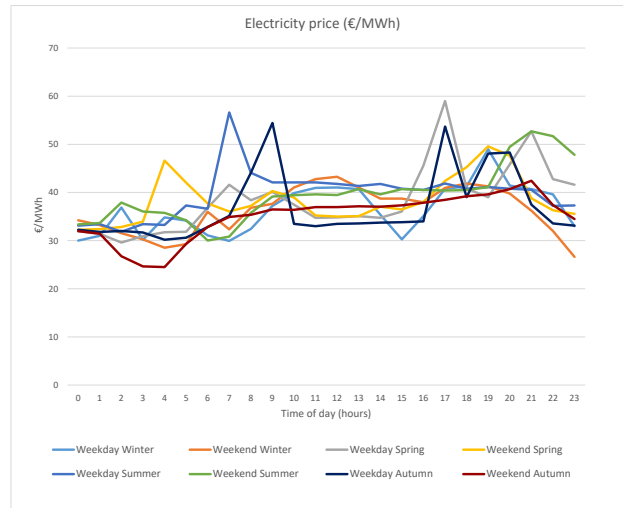


Fig. 6. Evolution of electricity prices for the 8 typical days, from Samsatli and Samsatli (2015).

The wind electric production is presented on figure 7. It varies hourly and seasonally. The hydrogen demand for the three clusters is presented in Figures 8 to 10. The demand is higher in summer and at 8am, 7pm and 10pm for the rest of the year. Figure 11 represents the difference between hydrogen production, assuming that all the electricity generated from wind turbines is used to produce hydrogen, with the conversion ratios presented in Table 1, and the demand for each hour of the year. The electricity production is not sufficient in summer during most part of the day, and at 7pm for a great part of the year.

In order to respond to the demand for these periods, two scenarios can be studied. Either electricity is imported and purchased from the grid, with an associated cost and is directly used to produce hydrogen. Or hydrogen is produced when there is a surplus of electricity (for example in winter) and is stored in a hydrogen tank. Then, stored hydrogen is delivered when there are electricity shortages, in summer or at 7pm for example. The optimization model can determine the balance between electricity imports or use of hydrogen storage, produced from local electricity.

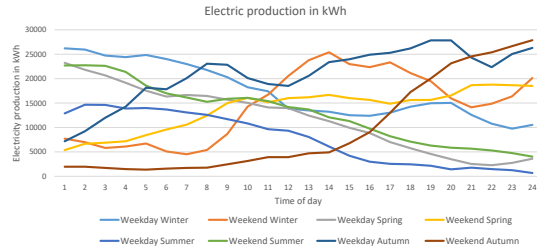


Fig. 7. Electricity production for the 8 typical days, from Samsatli and Samsatli (2015)

465 The storage is placed in the cluster C1, close to the hydrogen and electricity
 production. Different cases are considered, in order to evaluate the pertinence
 of the compressed gas storage model:

- case (0): Without hydrogen storage
- 470 • case (1): An incompressible storage, without any compression costs.
- case (2): A compressible hydrogen storage, with compression energy costs.
- case (3): A compressible hydrogen storage, with compression energy costs
 and a compressor CAPEX.

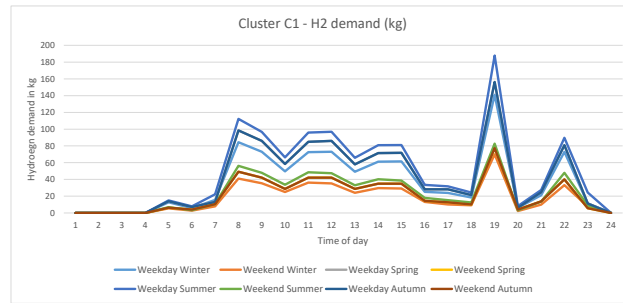
475 The characteristics of the modelling cases are presented in table 2. For
 each storage model, different pressure discretizations are introduced, allowing a
 higher precision of mechanical work computation. The error committed due to
 the linearization will be estimated and compared in order to assess the pertinence
 of the discretization.

480 For the compressed storage without any pressure discretization introduced,
 the electrical power for compression is 1.78 kWh/kg and it corresponds to an
 equivalent pressure of 77.8 bars (as if the gas was compressed at an equivalent
 pressure of 77.8 bars inside the storage). With one pressure introduced at 100
 bars, the electrical power is 1.47kWh/kg (equivalent pressure at 39.3 bars) for
 485 the first interval and 2.09kWh/kg (equivalent pressure at 147.3 bars) for the

Table 2

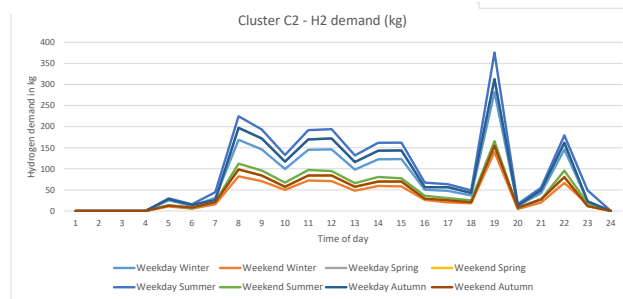
Characteristics of hydrogen storage

N' Case	Storage model	Pressure discretization	OPEX	CAPEX
1	Incompressible	-	-	500€/kg (Gorre et al., 2020)
2-a	Compressible	1-200 bars	1.78 kWh/kg	500€/kg
2-b		1-100-200 bars	Depends on pressure state	
2-c		1-66-133-200 bars	Depends on pressure state	
3-a	Compressible	1-200 bars	1.78 kWh/kg	500€/kg + 2000€/kW (compressor) (Klumpp, 2015; Aarnes et al., 2018)
3-b		1-100-200 bars	Depends on pressure state	
3-c		1-66-133-200 bars	Depends on pressure state	

**Fig. 8.** Hydrogen demand in the cluster C1 for the 8 typical days.

second interval. With two pressures introduced at 66 bars and 133 bars, the electrical power is 1.3kWh/kg (equivalent pressure at 26.5 bars), 1.9kWh/kg (equivalent pressure at 97.7 bars) and 2.15kWh/kg (equivalent pressure at 165 bars) for the first, second and third interval.

490

**Fig. 9.** Hydrogen demand in the cluster C2 for the 8 typical days.

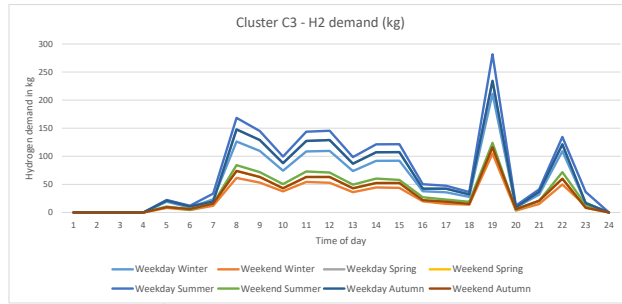


Fig. 10. Hydrogen demand in the cluster C3 for the 8 typical days.

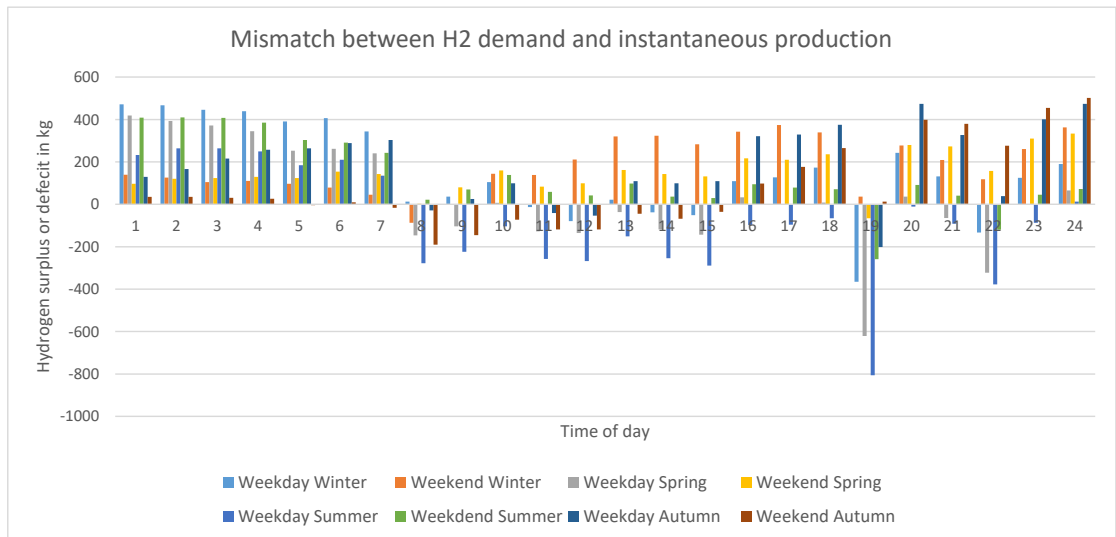


Fig. 11. Mismatch between hydrogen demand (aggregated) and instantaneous potential hydrogen production.

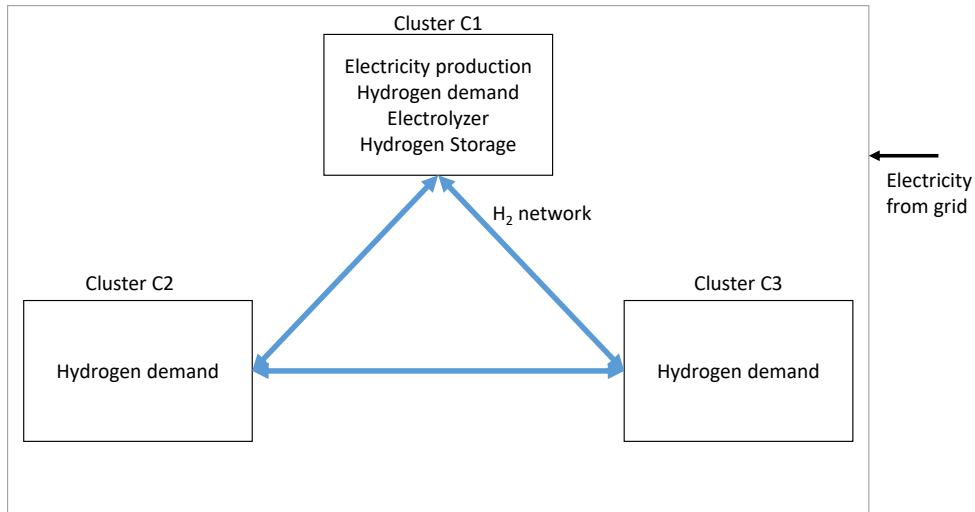


Fig. 12. Representation of the clusters C1, C2, C3 and of the potential hydrogen pathways. All clusters are 1km apart.

4.2. Design results

The case study is solved using CPLEX v12.7.1.0 solver (Nickel et al., 2021) on PC (Processor: Intel® Core™ i5-7200U CPU @ 2.50GHz – RAM: 16 Go – OS: Windows® 10). Table 3 presents the results: design of the electrolyzer, design of the hydrogen and CAPEX and OPEX for the different cases. The benefit of a hydrogen storage is clearly shown. Without any storage, the electrolyzer must be sized in order to supply the demand, specially for the peak demand for summer at 7pm. In order to respond to the demand, the power of the electrolyzer is 47MW, 4 times bigger than the scenarios with hydrogen storage. Thus, even if there are no investments associated to storage, CAPEX is higher. Moreover, as the electric production is not sufficient, electricity has to be bought from the grid, therefore OPEX is also higher. Including hydrogen storage reduces CAPEX and OPEX. It results in a smaller electrolyzer, around 12MW and independent of the hydrogen storage model. Indeed, hydrogen storage is used to shave the peak demand in hydrogen and avoid high electricity prices. When storage is used, the share of renewable electricity rises from 69% to almost 89%. Moreover, the total cost (CAPEX + OPEX) is reduced by around

2.4 when storage is used. CAPEX is higher for case 3, but storage modelling includes compressor CAPEX which can explain that. OPEX is also higher for
510 cases c because pressure discretization is finer. Thus, when hydrogen is stored at high pressure, compression cost is relatively higher for cases 2-c or 3-c than other cases (2-a, 3-a or 2-b and 3-b) with lower pressure discretization step.

Hydrogen storage behaviour depends on the daily demand for hydrogen and
515 renewable electricity production. The pressure inside the storage increases at the beginning of the day until 7pm, after which the storage is used to respond to the peak demand at 7pm (figure 13). Moreover, when electricity prices are high, for example at 5pm in spring, week-end, the electrolyzer is not running and hydrogen from storage is used to cover the needs. Conversely, the elec-
520 trolyzer works at full power when electricity is available (self-consumption) or cheaper (in summer, weekdays after 10am). Actually, no electricity is bought during winter and autumn because local production is sufficient. Renewable electricity is used to satisfy the demand in winter and autumn but also to fill the storage, anticipating the periods when the wind is not sufficient or miss-
525 ing. The hydrogen storage capacity is designed according to the peak demand in summer weekday and has a capacity of at least 2000 kg.(The difference between hydrogen demand and renewable hydrogen production is 2000 kg during a summer weekday (figure 11)). However, considering the day sequencing, the difference in a week is 3500 kg. Therefore, electricity still has to be bought from
530 the grid because the storage capacity is not enough to cover the total demand throughout the year. Actually, hydrogen capacity design results in a trade-off between CAPEX and OPEX. The depreciation period in the case study is set at 5 years but extending it can lead to greater investments and lower OPEX. When a value of 20 years is used, the storage is two times bigger (4000 kg) and
535 it results in a reduction of 38% of electricity bought from the grid.

For some cases ((2-c) and (3-c)), the optimality is not reached after 24 hours of computation. Indeed, these cases contain a lot of variables (binary and contin-

Table 3

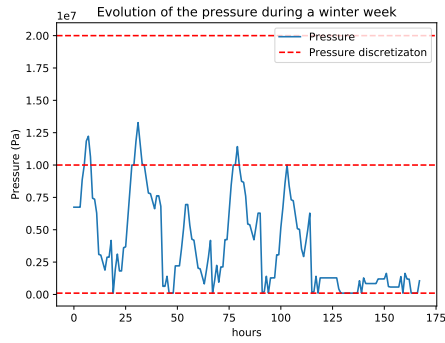
Design results for the different cases

Case	(0)	(1)	(2-a)	(2-b)	(2-c)	(3-a)	(3-b)	(3-c)
Electrolyzer power (kW)	46 954	12 020	12 018	12 019	12 019	12 018	12 258	12 019
Flow max Electrolyzer (kg/h)	845	216	216	216	216	216	218	216
Volume Storage (m^3)	(-)	(-)	125	125	125	125	130	128
Capacity storage (kg)	(-)	2038	2053	2052	2053	2053	2132	2100
Compressor (kW)	(-)	(-)	386	453	465	385	387	409
Compressor consumption (MWh)	(-)	(-)	909 237	881 201	826 071	1 077 838	949 507	866 203
CAPEX (M€)	27.48	11.03	11.04	11.04	11.04	11.81	11.97	11.91
Total OPEX (M€)	4.43	1.56	1.58	1.58	1.62	1.58	1.54	1.60
CAPEX + OPEX (M€)	31.91	12.59	12.62	12.61	12.65	13.39	13.51	13.52
Tolerance	0%	0%	0%	0%	0.10%	0%	0.10%	0.10%
Share of renewable electricity	68.7%	88.7%	88.6%	88.6%	88.3%	88.7%	88.9%	88.4%

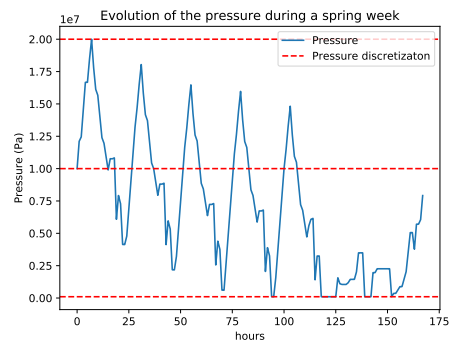
uous), making it difficult to solve them to optimality. Therefore, computational
540 difficulties are overcome by setting the design of the electrolyzer beforehand. Actually, the first results on cases 1, (2-a), (2-b) and (3-a) show that electrolyzer power does not depend on storage modelling and pressure discretization. Thus, the value of 12019kW obtained on cases 1, (2-a) and (3-a) is used on cases (2-c) and (3-c) to set the electrolyzer power and make the problem easier to solve.
545 The computation is stopped when the tolerance gap reaches 0.1%. Then, the actual energy compression can be computed in post-processing and be used to evaluate the error due to the linearization in section 4.3.

4.3. Compression work precision

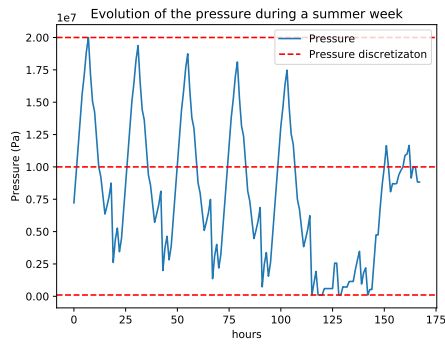
Because the compression costs are evaluated using a mean value for a certain
550 pressure interval, an approximation is realized. Actually, if the pressure interval is too wide, the mean value used for evaluating the compression cost can be far from the actual value. Particularly, when the storage is filled at low pressure, the compression work is over-estimated. In the opposite, when the storage is filled at high pressure, the compression work is under-estimated. Even if the
555 cumulative error can balance itself through the time periods, the error is also reflected on the compressor design. Therefore, introducing intermediate pressure will reduce pressure interval sizes and reduce this approximation. Moreover, as



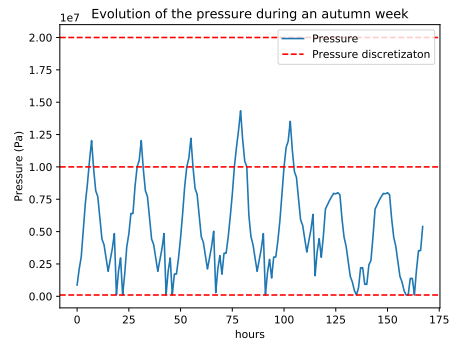
(a) Winter week



(b) Spring week



(c) Summer week



(d) Autumn week

Fig. 13. Evolution of the pressure inside the storage for the first week of each season. The red dot lines correspond to the discrete pressures. Results for case (3-b)

we can see in figure 13, the pressure inside a storage can pass from one interval pressure to the next when filling (for example from 85 bars to 105 bars in a hour during a summer week). The computation of the mechanical work uses both mean values of mechanical compression (before filling and after) as shown in equation (26). This attempts to reduce the error.

Results of compression work values are then compared to the exact values, without approximation. Storage pressure is computed from the ideal gas law (equation (19)), using the volume value and the hydrogen mass inside the storage obtained from the optimization. Then, mechanical compression work can be computed with the corresponding hydrogen flow at each hour without any approximation (equation (42)):

$$W_{electrolyzer,t}^{real} = L_t^{in} N C_p T \left(\frac{P_t^{\frac{\gamma-1}{N\gamma}}}{P_1} - 1 \right) \quad (42)$$

The actual design of the compressor can also be computed (equation (43)):

$$P_{electrolyzer}^{real} = \max_t \left(\frac{W_{electrolyzer,t}^{real}}{\delta_t} \right) \quad (43)$$

Results of the relative error due to the linearization are presented in table 4. The cases (0) and (1) are not included in the table because they do not include any hydrogen compressed storage model. The error committed on compression consumption decreases with the introduction of intermediate pressure, from 13% to 10% concerning the total mechanical compression energy (for both cases (2-x) and (3-x)). The error on energy compression is relatively the same for the storage (2-a) and (2-b) (13% and a difference of nearly 114,000MWh) but the introduction of an intermediate pressure at 100 bars reduces the total energy consumption by 3%. Supposing an electricity price of 40€/MWh, it results in a cost savings of more than 1M€. (Note that in this case, local grid electricity is available from local production, that explains why there is no difference in OPEX in table 3 between case (2-a) and case (2-b), higher electricity consumption is absorbed by the local production). For compressor design, the error is

not relevant for cases (2-x) because compressor CAPEX is not considered, and
585 has no influence on the optimization. For compression design, introducing a
pressure discretization improves the precision, from 10% to 4% or 7% for the
case 3.

Figure 14 compares the compression work obtained from optimization (x-
590 axis) and with the value obtained from post-calculation (y-axis). The post-
computed value uses the exact pressure value inside the storage to compute the
enthalpy compression, then the compression mass flow (get from optimization)
is used to compute the energy compression. Three cases are presented on the
figure: cases (2-a), (2-b) and (2-c). For instance for the case (2-b), one interme-
595 diate pressure is introduced (100 bars) and three discrete values are available
for enthalpy compression: one for a pressure state below 100 bars, one for a
pressure state above 100 bars and one intermediate value (if the binary for pres-
sure interval changes between two periods). These values are computed from
equation (26) and are used in the optimization problem to compute compression
600 work (x-axis).

The gap between the orange line 'y=x' and the blue crosses shows the preci-
sion on the compression work calculation. The error is lower as the blue cross
gets closer to the orange line. If the blue cross is below the orange line, then
the compression work is over-estimated. If the blue is above, the compression
605 work is under-estimated. This figure shows that the compression work is over-
estimated as the blue crosses are most-of-time below the line 'y=x'. Hence, the
discrete value for enthalpy compression over-estimates its real value. Actually,
increasing the number of discrete pressure (case 2-c) increases the precision on
computation of the compression enthalpy and the blue crosses get closer to the
610 line 'y=x'. The approximation of the pressure in the storage is better estimated,
hence compression works also, particularly for high values of energy compression.
Moreover, when the compression CAPEX is included (3-a, 3-b and 3-c),
the error on compressor design decreases with the number of intermediate pres-
sure. The error is only of 7% for the case (3-c) and 4% for the case (3-b). Using

615 at least one intermediate discrete pressure seems to be enough to catch the actual size of the compressor and to provide a good estimation of the compressor consumption.

However, the tractability challenge must not be forgotten. If a great number
620 of discrete pressures are introduced, the number of variables rises sharply. For each time period and pressure interval, two continuous variables and one binary variable are defined for pressure characterization. Thus, at a constant number of periods, the number of variables increases as the number of pressure steps are specified. The problem could become quickly intractable in terms of solution
625 time or finding a solution. Therefore, a solution methodology must be established in order to compute complex case studies. The proposed methodology is composed of two steps:

1. The first step consists of solving the problem with a reduced number of pressure steps. Electrolyzers (or any conversion systems) are designed
630 and an electric power is proposed. A certain volume of gas storage is also designed.
2. The second step uses results from step 1. Values of conversion system power and gas storage capacities are set, from step 1 results. It helps in reducing the size of the problem and a solution is found faster and easier.

635 For example, for the cases 2-c and 3-c, without any predesign result, the optimality gap is stuck at about 30% after more than 24 hours of computing time. The duration is reduced to around 18,000 seconds (CPU time), showing the interest of the methodology.

5. Perspectives

640 A comprehensive modelling structure for hydrogen generation, transport and storage optimization with a detailed model of compressed gas storage has been presented, but further improvements and works will be introduced to the model, based on this formulation:

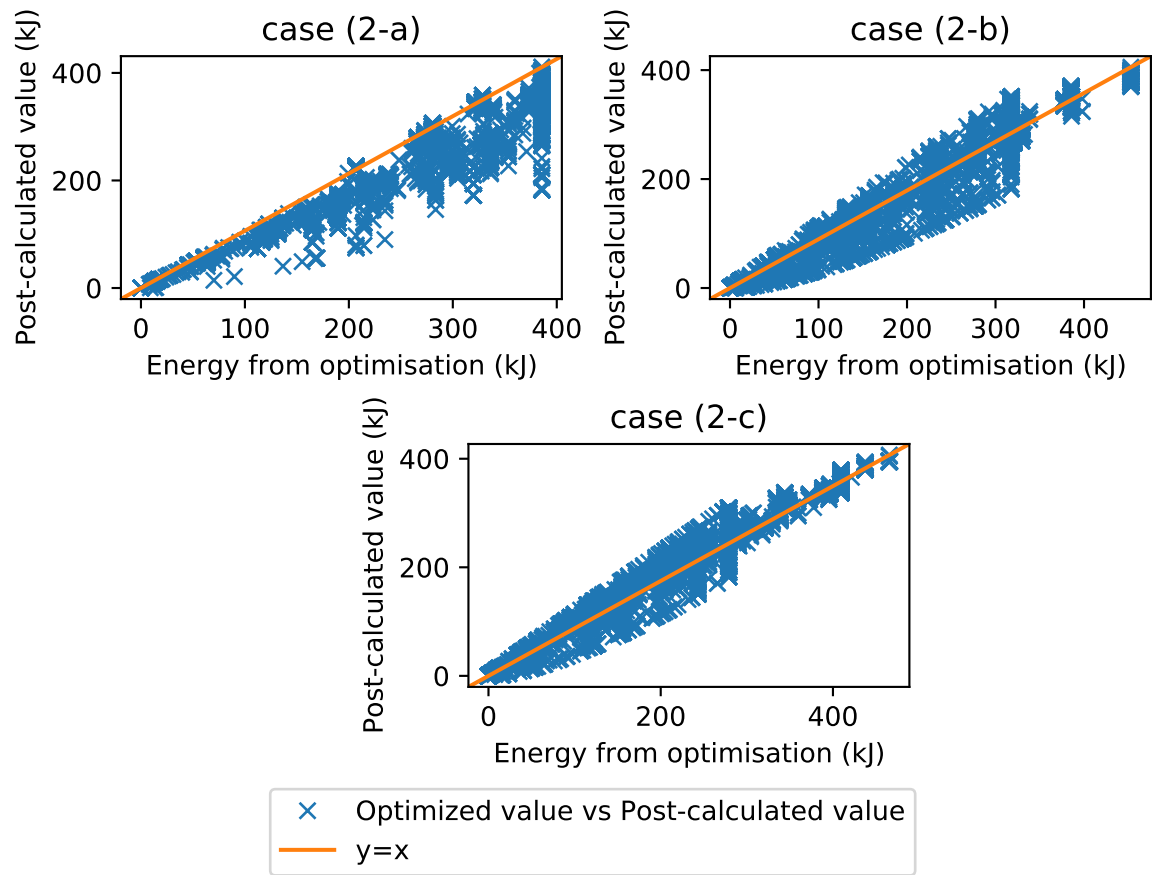


Fig. 14. Comparison of the mechanical work obtained by the optimization (x-axis) versus the post-calculated value (y-axis)

Table 4

Error committed on mechanical compression and compressor design for the different storages

Case	(2-a)	(2-b)	(2-c)	(3-a)	(3-b)	(3-c)
Compressor (kW)	386	453	465	385	387	409
Compressor - real (kW)	411	405	406	422	371	379
Relative error (%)	6%	11%	13%	10%	4%	7%
Annual compressor consumption (MWh)	909 237	881 201	826 071	1 077 838	949 507	866 203
Annual compressor consumption - real (MWh)	795 526	764 601	743 455	901 166	848 441	783 136
Relative error (%)	13%	13%	10%	16%	11%	10%
CAPEX error (%)	0.00%	0.00%	0.00%	0.61%	-0.27%	-0.52%
OPEX error (%)	-0.38%	-0.14%	-0.07%	-0.38%	-0.25%	-0.08%

- 645 • Part-load modelling. Actually, systems as electrolyzers or fuel cells do not operate at nominal performance 100% of the time. They can operate at part-load performance and see their efficiency be degraded or improved, compared to nominal performance. Hence, this aspect should be considered in multi-period problems, especially when intermittent energies are used.
- 650 • Tractability challenge. Computational issues can be observed because of the great number of continuous and binary variables and the considered time step here (1 hour). Increased time step durations could be studied, but this would impact the accuracy of intermittent electricity production data. A formulation in typical days could also be studied, but with particular attention on day sequencing in order to catch the storage dynamics through several days.

655
- 660 • Energy (heat) and mass networks will be designed simultaneously. Indeed, the presence of conversion systems (such as electrolyzers) couples all the aspects of the problem. For a better comprehensive study of a territory, a systemic view of the problem will be carried out. It will lead to better solutions than treating each aspect (water, hydrogen, energy, heat, ...) separately.
- Waste heat valorization at the compressor intercooler. In this way and

thanks to the new compressed gas storage model, compressor power can
665 be estimated. Therefore, the compressor intercooling needs can also be es-
timated, and this waste heat could be recovered and valorized for thermal
needs. This point is relevant to the previous one.

- An industrial park is a complex area of study. There can be competition
in the use of resources, but also competition between industrial actors.
670 Indeed, the model presented in this article assumes that each actor coop-
erates with each other and do not pay for the resource. It corresponds
to a cooperative-game. However, in real life, industrials actors will seek
its best economic interest, and will pay for the resource. As well, the dis-
tributor or producer will invest in the network and must be remunerated
675 for the service. A competition appears between producer and industrial
buyers appears. This will lead to non-cooperative scheme. Methodology
will be investigated to model such kind of transaction.

6. Conclusions and future work

This paper presents a multi-period optimization linear model for the de-
680 sign of mass networks, including conversion systems and compressed gas stor-
ages. A generic model of conversion system is proposed based on its efficiency.
A linear model of compressed gas storages is proposed based on pressure dis-
cretization, allowing the design of the compressor. The compressed costs can
be computed and included into the objective function, the minimization of to-
685 tal costs (CAPEX + OPEX). The model is applied to a hydrogen case study
inspired from the literature. The electricity generated from wind turbines is
used to produce hydrogen to fulfill the hydrogen demands. Mass networks, elec-
trolyzers and hydrogen (compressed) storages are designed. A comparison is
done between results from optimization (linear model of compressed gas stor-
690 ages) and actual model of compressed gas storages. It shows that the electric
consumption cannot be neglected in this case and the compressor power influ-
ences the solution. The approximation due to the linearization decreases as the

pressure discretization is finer. However, the complexity of the model increases with the number of discrete pressures and the problem can become intractable, specially when a great number of periods or pressure steps are considered. A methodology based on pre-design is used in order to solve finer compressed gas storage model in an acceptable solution time. Numerous additions to the model have also been identified and can help us to increase the model reality: part-load efficiency, coupling mass and energy networks, waste heat valorization at the compressor and modelling of competitive and individual interests of each actor and tractability challenge.

7. Acknowledgment

The authors acknowledge the ADEME institute for their financing support in the EPIFLEX project.

705 Nomenclature

Subscripts and superscripts

c	Cluster
cs	Thermodynamic energy conversion system
i	Sink
710 j	Source
m	Mass network
p	Path
r	Resource
s	Storage
715 t	Time period
v	Variable

Sets

	M_{net}	Mass networks
	C	Clusters
720	I	Sources
	J	Sinks
	P	Paths
	R	Resources
	S	Storages
725	SC	Conversion systems
	T	Time periods

Parameters

	δ_p	Arbitrary direction of the path p
	γ	Constant heat capacity
730	Ω	Big number
	$w_{s,t}^{comp}$	Compression work of the gas storage s
	$w_{c,s,p}$	Mean value of enthalpy compression in the pressure interval p
	C_t^e	Electricity price at time t
	C_s^p	Variable part for compressor cost
735	C_{cs}^u	Fixed part for conversion system investment cost
	C_p^u	Nominal cost per distance for a pipe
	C_s^u	Fixed part for storage investment cost
	C_i^v	Cost of material disposal in sink i

	C_j^v	Cost of material of source j
740	C_{cs}^v	Variable part for conversion system investment cost
	C_s^v	Variable part for storage investment cost
	d_p	Length of a pipe p
	EC_t	Total electricity consumption at time t
	$EP_{c,t}^c$	Electricity production inside a cluster c at time t
745	EP_t^{limit}	Limit of sold electricity to the grid at time t
	$EP_t^{res,in}$	Electricity bought to the grid at time t
	$EP_t^{res,out}$	Electricity sold to the grid at time t
	EP_t	Total electricity production at time t
	$G_{c,i_r,t}$	Mass flow rate demand
750	$L_{c,j_f,t}^{cs}$	variable mass flow of the reference source j_f defining a conversion system cs at time t
	$L_{c,j_r,t}$	Mass flow rate availability
	M_g	Molar mass of the gas g
	N	Number of pressure stages
755	N_y	Number of operating years
	$P_{cs,t}^{cs}$	Electrical consumption or production of the conversion system cs at time t
	P_{cs}^{cs}	Electrical power of the conversion system cs
	P_s	Compressor power of the storage s
760	$P_{s,i}$	Discrete pressure of the interval i

	r_a	Actualization ratio
	$rs_{j/i}$	conversion system efficiency associated to source/sink j/i
	T_s	Temperature inside the storage
	V_{i_m, j_m}	Volume of the gas storage $(i_m, j_m) = s$
765	<i>Continuous variables</i>	
	$C_{c, i_r, t}^v$	Mass flow rate entering into a variable sink
	$L_{c, i_j, r, t}^v$	Mass flow rate between a variable source and a sink
	$L_{c, j_r, t}^v$	Mass flow rate leaving a variable source
	$L_{c, s, t, p_s}^{p, in, after/before}$	Mass flow rate entering into the discretized gas storage at the
770		pressure
	$L_{p, t}^{path}$	Mass flow rate through the path p
	$L_{c, i_j, r, t}$	Mass flow rate between a source and a sink
	$Max_S_{c, s, r}$	Maximum amount of resource r stored
	$Min_S_{c, s, r}$	Minimum amount of resource r stored
775	$S_{c, s, r, t}$	Amount of resource r stored at time t
	<i>Integer variables</i>	
	b_{cs}^b	Binary indicating if a conversion system is used or not
	$b_{c, j_r, t}^{in}$	Binary indicating if the storage is filling
	$b_{c, i_r, t}^{out}$	Binary indicating if the storage is emptying
780	$b_{s, t, p}^P$	Binary indicating the pressure interval p inside the gas storage s
	$b_{c, s, r, t}^S$	Binary indicating if the storage is used
	b_p	Binary indicating if a path p is used

Abbreviations

CAPEX Capital expenditure

785 MILP Mixed-integer linear programming

OPEX Operating expenditure

References

Eurostat, Renewable energy in the EU in 2018, Technical Report, 2020.

URL: <https://ec.europa.eu/eurostat/documents/2995521/10335438/8-23012020-AP-EN.pdf/292cf2e5-8870-4525-7ad7-188864ba0c29>.

790 A. Kusko, J. DeDad, Short-term, long-term, energy storage methods for standby electric power systems, in: Conference Record - IAS Annual Meeting (IEEE Industry Applications Society), volume 4, IEEE, 2005, pp. 2672–2678. URL: <http://ieeexplore.ieee.org/document/1518837/>. doi:10.1109/IAS.2005.1518837.

S. C. Smith, P. K. Sen, B. Kroposki, Advancement of energy storage devices and applications in electrical power system, in: IEEE Power and Energy Society 2008 General Meeting: Conversion and Delivery of Electrical Energy in the 21st Century, PES, IEEE, 2008, pp. 1–8. URL: <http://ieeexplore.ieee.org/document/4596436/>. doi:10.1109/PES.2008.4596436.

800 S. B. Walker, U. Mukherjee, M. Fowler, A. Elkamel, Benchmarking and selection of Power-to-Gas utilizing electrolytic hydrogen as an energy storage alternative, International Journal of Hydrogen Energy 41 (2016) 7717–7731. URL: <https://linkinghub.elsevier.com/retrieve/pii/S0360319915022570>. doi:10.1016/j.ijhydene.2015.09.008.

M. Götz, J. Lefebvre, F. Mörs, A. McDaniel Koch, F. Graf, S. Bajohr, R. Reimert, T. Kolb, Renewable Power-to-Gas: A technological and economic review, Renewable Energy 85 (2016) 1371–1390. URL: <https://doi.org/10.1016/j.renene.2015.10.088>.

- //linkinghub.elsevier.com/retrieve/pii/S0960148115301610. doi:10.
810 1016/j.renene.2015.07.066.
- K. Mazloomi, C. Gomes, Hydrogen as an energy carrier: Prospects and challenges, Renewable and Sustainable Energy Reviews 16 (2012) 3024–3033. URL: <https://linkinghub.elsevier.com/retrieve/pii/S1364032112001220>. doi:10.1016/j.rser.2012.02.028.
- 815 Z. Abdin, C. J. Webb, E. M. Gray, Modelling and simulation of a proton exchange membrane (PEM) electrolyser cell, International Journal of Hydrogen Energy 40 (2015) 13243–13257. URL: <https://linkinghub.elsevier.com/retrieve/pii/S0360319915019321>. doi:10.1016/j.ijhydene.2015.07.129.
- 820 Z. Abdin, C. J. Webb, E. M. A. Gray, Modelling and simulation of an alkaline electrolyser cell, Energy 138 (2017) 316–331. URL: <https://linkinghub.elsevier.com/retrieve/pii/S0360544217312288>. doi:10.1016/j.energy.2017.07.053.
- F. Barbir, PEM electrolysis for production of hydrogen from renewable energy sources, Solar Energy 78 (2005) 661–669. URL: <https://linkinghub.elsevier.com/retrieve/pii/S0038092X04002464>. doi:10.1016/j.solener.2004.09.003.
- 830 E&E Consultant, HESPUL, Solagro, Etude portant sur l’hydrogène et la méthanation comme procédé de valorisation de l’électricité excédentaire, Technical Report, 2014. URL: www.grtgaz.com/fileadmin/engagements/documents/fr/Power-to-Gas-etude-ADEME-GRTgaz-GrDF-complete.pdf.
- K. Onda, T. Murakami, T. Hikosaka, M. Kobayashi, R. Notu, K. Ito, Performance Analysis of Polymer-Electrolyte Water Electrolysis Cell at a Small-Unit Test Cell and Performance Prediction of Large Stacked Cell, Journal of The Electrochemical Society 149 (2002) A1069. URL: <https://iopscience.iop.org/article/10.1149/1.1492287>. doi:10.1149/1.1492287.

- M. J. Khan, M. T. Iqbal, Dynamic modeling and simulation of a small wind-fuel cell hybrid energy system, *Renewable Energy* 30 (2005) 421–439. URL: <https://linkinghub.elsevier.com/retrieve/pii/S0960148104002381>. doi:10.1016/j.renene.2004.05.013.
- 840
- S. Busquet, C. E. Hubert, J. Labbé, D. Mayer, R. Metkemeijer, A new approach to empirical electrical modelling of a fuel cell, an electrolyser or a regenerative fuel cell, *Journal of Power Sources* 134 (2004) 41–48. URL: <https://linkinghub.elsevier.com/retrieve/pii/S0378775304002472>. doi:10.1016/j.jpowsour.2004.02.018.
- 845
- S. Kélouwani, K. Agbossou, R. Chahine, Model for energy conversion in renewable energy system with hydrogen storage, *Journal of Power Sources* 140 (2005) 392–399. URL: <https://linkinghub.elsevier.com/retrieve/pii/S0378775304008821>. doi:10.1016/j.jpowsour.2004.08.019.
- 850
- H. Görgün, Dynamic modelling of a proton exchange membrane (PEM) electrolyzer, *International Journal of Hydrogen Energy* 31 (2006) 29–38. URL: <https://linkinghub.elsevier.com/retrieve/pii/S0360319905000868>. doi:10.1016/j.ijhydene.2005.04.001.
- D. S. Falcão, A. M. Pinto, A review on PEM electrolyzer modelling: Guidelines for beginners, *Journal of Cleaner Production* 261 (2020) 121184. URL: <https://linkinghub.elsevier.com/retrieve/pii/S0959652620312312>. doi:10.1016/j.jclepro.2020.121184.
- 855
- M. Carmo, D. L. Fritz, J. Mergel, D. Stolten, A comprehensive review on PEM water electrolysis, *International Journal of Hydrogen Energy* 38 (2013) 4901–4934. URL: <https://linkinghub.elsevier.com/retrieve/pii/S0360319913002607>. doi:10.1016/j.ijhydene.2013.01.151.
- 860
- P. Olivier, C. Bourasseau, P. B. Bouamama, Low-temperature electrolysis system modelling: A review, *Renewable and Sustainable Energy Reviews* 78 (2017) 280–300. URL: <https://linkinghub.elsevier.com/retrieve/pii/S136403211730432X>. doi:10.1016/j.rser.2017.03.099.
- 865

- F. Marangio, M. Pagani, M. Santarelli, M. Cali, Concept of a high pressure PEM electrolyser prototype, *International Journal of Hydrogen Energy* 36 (2011) 7807–7815. URL: <https://linkinghub.elsevier.com/retrieve/pii/S0360319911001364>. doi:10.1016/j.ijhydene.2011.01.091.
- 870 M. E. Lebbal, S. Lecœuche, Identification and monitoring of a PEM electrolyser based on dynamical modelling, *International Journal of Hydrogen Energy* 34 (2009) 5992–5999. URL: <https://linkinghub.elsevier.com/retrieve/pii/S0360319909002018>. doi:10.1016/j.ijhydene.2009.02.003.
- J. Nie, Y. Chen, S. Cohen, B. D. Carter, R. F. Boehm, Numerical and
875 experimental study of three-dimensional fluid flow in the bipolar plate of a PEM electrolysis cell, *International Journal of Thermal Sciences* 48 (2009) 1914–1922. URL: <https://linkinghub.elsevier.com/retrieve/pii/S1290072909000386>. doi:10.1016/j.ijthermalsci.2009.02.017.
- J. Nie, Y. Chen, Numerical modeling of three-dimensional two-phase gas-
880 liquid flow in the flow field plate of a PEM electrolysis cell, *International Journal of Hydrogen Energy* 35 (2010) 3183–3197. URL: <https://linkinghub.elsevier.com/retrieve/pii/S0360319910001217>. doi:10.1016/j.ijhydene.2010.01.050.
- A. Awasthi, K. Scott, S. Basu, Dynamic modeling and simulation of a proton exchange membrane electrolyzer for hydrogen production,
885 *International Journal of Hydrogen Energy* 36 (2011) 14779–14786. URL: <https://linkinghub.elsevier.com/retrieve/pii/S0360319911006343>. doi:10.1016/j.ijhydene.2011.03.045.
- R. García-Valverde, N. Espinosa, A. Urbina, Simple PEM water electrolyser
890 model and experimental validation, *International Journal of Hydrogen Energy* 37 (2012) 1927–1938. URL: <https://linkinghub.elsevier.com/retrieve/pii/S0360319911021380>. doi:10.1016/j.ijhydene.2011.09.027.
- P. Gabrielli, B. Flamm, A. Eichler, M. Gazzani, J. Lygeros, M. Mazzotti, Modeling for optimal operation of PEM fuel cells and electrolyzers, in: *EEEIC 2016*

895 - International Conference on Environment and Electrical Engineering, IEEE,
2016, pp. 1–7. URL: <http://ieeexplore.ieee.org/document/7555707/>.
doi:10.1109/EEEIC.2016.7555707.

M. Reuß, L. Welder, J. Thürauf, J. Linßen, T. Grube, L. Schewe, M. Schmidt,
D. Stolten, M. Robinius, Modeling hydrogen networks for future en-
900 ergy systems: A comparison of linear and nonlinear approaches, *Internation-
al Journal of Hydrogen Energy* 44 (2019) 32136–32150. URL: [https://
linkinghub.elsevier.com/retrieve/pii/S0360319919338625](https://linkinghub.elsevier.com/retrieve/pii/S0360319919338625). doi:10.
1016/j.ijhydene.2019.10.080.

P. L. Zervas, H. Sarimveis, J. A. Palyvos, N. C. Markatos, Model-based optimal
905 control of a hybrid power generation system consisting of photovoltaic arrays
and fuel cells, *Journal of Power Sources* 181 (2008) 327–338. URL: [https://
linkinghub.elsevier.com/retrieve/pii/S0378775307025736](https://linkinghub.elsevier.com/retrieve/pii/S0378775307025736). doi:10.
1016/j.jpowsour.2007.11.067.

L. Li, H. Manier, M. A. Manier, Hydrogen supply chain network design: An
910 optimization-oriented review, *Renewable and Sustainable Energy Reviews*
103 (2019) 342–360. URL: [https://linkinghub.elsevier.com/retrieve/
pii/S1364032118308633](https://linkinghub.elsevier.com/retrieve/pii/S1364032118308633). doi:10.1016/j.rser.2018.12.060.

D. Yue, F. You, S. W. Snyder, Biomass-to-bioenergy and bio-
fuel supply chain optimization: Overview, key issues and challenges,
915 *Computers and Chemical Engineering* 66 (2014) 36–56. URL: [https://
linkinghub.elsevier.com/retrieve/pii/S0098135413003670](https://linkinghub.elsevier.com/retrieve/pii/S0098135413003670). doi:10.
1016/j.compchemeng.2013.11.016.

M. Moreno-Benito, P. Agnolucci, L. G. Papageorgiou, Towards a sus-
tainable hydrogen economy: Optimisation-based framework for hydrogen
920 infrastructure development, *Computers and Chemical Engineering* 102
(2017) 110–127. URL: [https://linkinghub.elsevier.com/retrieve/pii/
S0098135416302666](https://linkinghub.elsevier.com/retrieve/pii/S0098135416302666). doi:10.1016/j.compchemeng.2016.08.005.

- S. A. Van Den Heever, I. E. Grossmann, A strategy for the integration of production planning and reactive scheduling in the optimization of a hydrogen supply network, *Computers and Chemical Engineering* 27 (2003) 1813–1839. URL: <https://linkinghub.elsevier.com/retrieve/pii/S0098135403001583>. doi:10.1016/S0098-1354(03)00158-3.
- M. Martín, I. E. Grossmann, Energy optimization of hydrogen production from lignocellulosic biomass, *Computers and Chemical Engineering* 35 (2011) 1798–1806. URL: <https://linkinghub.elsevier.com/retrieve/pii/S0098135411000925>. doi:10.1016/j.compchemeng.2011.03.002.
- A. Almansoori, N. Shah, Design and operation of a future hydrogen supply chain: Snapshot model, *Chemical Engineering Research and Design* 84 (2006) 423–438. URL: <https://linkinghub.elsevier.com/retrieve/pii/S0263876206729185>. doi:10.1205/cherd.05193.
- A. Almansoori, N. Shah, Design and operation of a future hydrogen supply chain: Multi-period model, *International Journal of Hydrogen Energy* 34 (2009) 7883–7897. URL: <https://linkinghub.elsevier.com/retrieve/pii/S036031990901235X>. doi:10.1016/j.ijhydene.2009.07.109.
- L. Li, H. Manier, M. A. Manier, Integrated optimization model for hydrogen supply chain network design and hydrogen fueling station planning, *Computers and Chemical Engineering* 134 (2020) 106683. URL: <https://linkinghub.elsevier.com/retrieve/pii/S0098135419305757>. doi:10.1016/j.compchemeng.2019.106683.
- G. A. Chahla, A. Zoughaib, Agent-based conceptual framework for energy and material synergy patterns in a territory with non-cooperative governance, *Computers and Chemical Engineering* 131 (2019) 106596. URL: <https://linkinghub.elsevier.com/retrieve/pii/S0098135419306842>. doi:10.1016/j.compchemeng.2019.106596.
- S. Samsatli, N. J. Samsatli, A general spatio-temporal model of energy systems with a detailed account of transport and storage, *Com-*

- puters & Chemical Engineering 80 (2015) 155–176. URL: <https://linkinghub.elsevier.com/retrieve/pii/S0098135415002008>. doi:10.1016/j.compchemeng.2015.05.019.
- 955 H. Barthelemy, M. Weber, F. Barbier, Hydrogen storage: Recent improvements and industrial perspectives, *International Journal of Hydrogen Energy* 42 (2017) 7254–7262. URL: <https://linkinghub.elsevier.com/retrieve/pii/S0360319916305559>. doi:10.1016/j.ijhydene.2016.03.178.
- 960 F. Ruiming, Multi-objective optimized operation of integrated energy system with hydrogen storage, *International Journal of Hydrogen Energy* 44 (2019) 29409–29417. URL: <https://linkinghub.elsevier.com/retrieve/pii/S036031991930792X>. doi:10.1016/j.ijhydene.2019.02.168.
- 965 S. Ghazouani, A. Zoughaib, S. Le Bourdier, An MILP model for the simultaneous design of mass and heat networks of a collaborative eco-industrial park, in: *Computer Aided Chemical Engineering*, volume 40, 2017, pp. 1939–1944. URL: <https://linkinghub.elsevier.com/retrieve/pii/B9780444639653503251>. doi:10.1016/B978-0-444-63965-3.50325-1.
- 970 S. Ghazouani, Linear optimization models for the simultaneous design of mass and heat networks of an eco-industrial park, Ph.D. thesis, Université Paris sciences et lettres, 2016.
- 975 W. Won, H. Kwon, J.-H. Han, J. Kim, Design and operation of renewable energy sources based hydrogen supply system: Technology integration and optimization, *Renewable Energy* 103 (2017) 226–238. URL: <https://linkinghub.elsevier.com/retrieve/pii/S0960148116310072>. doi:10.1016/j.renene.2016.11.038.
- J. D. Jacobs, Economic Modeling of Cost Effective Hydrogen Production From Water Electrolysis by Utilizing Iceland’s Regulating Power Market, Ph.D. thesis, 2016.

- J. Gorre, F. Ruoss, H. Karjunen, J. Schaffert, T. Tynjälä, Cost benefits of opti-
980 mizing hydrogen storage and methanation capacities for Power-to-Gas plants
in dynamic operation, *Applied Energy* 257 (2020) 113967. URL: <https://linkinghub.elsevier.com/retrieve/pii/S030626191931654X>. doi:10.1016/j.apenergy.2019.113967.
- F. Klumpp, Potential for large scale energy storage technologies - Com-
985 parison and ranking including an outlook to 2030, *Energy Procedia* 73
(2015) 124–135. URL: <https://linkinghub.elsevier.com/retrieve/pii/S1876610215014277>. doi:10.1016/j.egypro.2015.07.659.
- J. Aarnes, M. Eijgelaar, E. Hektor, Hydrogen as an Energy Carrier: An Evalua-
tion of Emerging Hydrogen Value Chains, Technical Report, DNV-GL, 2018.
990 URL: <https://www.h2knowledgecentre.com/content/policypaper614>.
- S. Nickel, C. Steinhardt, H. Schlenker, W. Burkart, M. Reuter-Oppermann,
IBM ILOG CPLEX Optimization Studio, in: *Angewandte Optimierung
mit IBM ILOG CPLEX Optimization Studio*, Springer Berlin Heidelberg,
Berlin, Heidelberg, 2021, pp. 9–23. URL: http://link.springer.com/10.1007/978-3-662-62185-1_2.
995 doi:10.1007/978-3-662-62185-1_2.